Supporting Information

Counterion-induced Crystallization of Intermetalloid *Matryoshka* Clusters $[Sb@Pd_{12}@Sb_{20}]^{3-,4-}$

Zhenyu Li,[a,b] Huapeng Ruan,[a,b] Lulu Wang [a,b] and Li Xu*[a]

a. Department State Key Laboratory of Structural Chemistry, Institution Fujian Institute of Research on the Structure of Matter Chinese Academy of Sciences, Fuzhou, Fujian 350002, P. R. China.

b. University of the Chinese Academy of Science, Beijing,100049, P.R. China

E-mail: xli@fjirsm.ac.cn.

S1 Experimental Section

All manipulations were carried out under argon using standard Schlenk-line and glovebox techniques. Ethylenediamine (Acros, 99%) was distilled over sodium metal and stored in a gastight Schlenk under argon in the glovebox. 18-crown-6 (1,4, 7,10, 13, 16-hexaoxacyclooctadecane, Alfa-Aesar, 99 %) was dried by refluxing over sodium metal in diethylether and recrystallized from dry n-hexanes. Toluene was dried with potassium-sodium alloy and then stored in the glovebox. $Pd(PPh_3)_4$ (Alfa-Aesar, 98%) was used as received. Precursors with nominal composition KSb[1] was synthesized by heating the corresponding mixtures of elements (K :+99 %; Sb: 99.999 %, all from Strem) at 750℃ for two days in sealed niobium containers that were jacketed in evacuated fused-silica ampoules. ESR spectra were recorded on a Bruker ER-420 spectrometer with a 100 kHz magnetic field in the X band at room temperature in solid state sample(ground single crystal). DFT calculations were performed using the GAUSSIAN 09 program package (Revision D.01)[2] and crystal structure parameters. DFT calculations were carried out using the (U)B3LYP functional, that is, Beck's hybrid three-parameter exchange functional[3] with the Lee-Yang-Parr correlation functional.[4] In these calculations, the solvent effects were taken into account by the Polarizable Contiuum Model (PCM).[5] The natural atomic orbital(NAO) analyses were calculated by the NBO 3.1 module embedded in Gaussian 09 program. The analyses of frontier molecular orbitals and spin densities were performed by Multiwfn[6], which is a multifunctional wavefunction analysis program developed by Lu et. al. and can be freely downloaded.

Synthesis of $[Sb_{20}Pd_{12}@Sb][K(18\text{-crown-}6)]_4$ (**1**): The binary alloy with the nominal composition KSb (36 mg, 0.230 mmol) and 18-crown-6(167 mg, 0.632 mmol) were dissolved in 2 mL ethylenediamine and stirred for 3 hours at room temperature, resulting in a light brown solution, to which $Pd(PPh_3)_4$ (30 mg, 0.026 mmol) was added. The resulting solution was stirred for 10 minutes at room temperature and turned brown. The resulting brown solution was filtered *via* a glass fiber pipette and the filtrate was layered with toluene (8 ml). Black, plate crystals of **1**(3 mg, 6% based on KSb) were obtained after 10 days.

Synthesis of $[Sb_{20}Pd_{12}@Sb][K(2,2,2\text{-cryptand})]_3$ (**2**): The binary alloy with the nominal composition KSb (40 mg, 0.249 mmol) and 2,2,2-crypt (114 mg, 0.303 mmol) were dissolved in 2 mL ethylenediamine and stirred for 3 hours at room temperature, resulting in a dark red solution, to which $Pd(PPh_3)_4$ (37 mg, 0.032 mmol) was added. The resulting solution was stirred for 10 minutes at room temperature and was filtered *via* a glass fiber pipette. The filtrate was layered with toluene (8 ml). Black, needle-like crystals of **2**(5 mg, 8% based on KSb) were obtained after 10 days.

Single crystal X-ray diffraction data were collected on a Rigaku Mercury CCD diffractometer equipped with a graphite-monochromated Mo Kα radiation (λ = 0.71073 Å) at 293 K for **1** and 293K for **2**. The structure was solved by direct methods and refined on F2 against all reflections using the SHELXTL V6.21 package.[7] Crystallographic data for $[Sb_{20}Pd_{12}@Sb][K(18\text{-crown-}6)]_4$ (**1**): Cubic, $Pa\bar{3}$, a = 29.590(2) Å, V = 25909(3) Å^3, Z = 4, R_1/wR_2 = 7.45/18.94% for the observed data (I ≥2σ(I)), R_1/wR_2 = 7.59/19.06% for all data. (Platon SQUEEZE has been implemented.) Crystallographic data for $[Sb@Pd_{12}@Sb_{20}][K(2,2,2\text{-cryptand})]_3$ (**2**): Hexagonal, $R\bar{3}c$, a = 23.635(6) Å, c = 34.987(13) Å, V = 16927(9) Å^3, Z = 6, R_1/wR_2 = 7.39/16.99% for the observed data ($I \geq 2\sigma(I)$), R_1/wR_2 = 7.60/17.18% for all data. (Platon SQUEEZE has been implemented.) CCDC 1511293 for 1 and CCDC 1511294 for 2 contain the supplementary crystallographic data for this paper. These data can be obtained free of charge from the Cambridge Crystallographic Data Centre via *www.ccdc.cam.ac.uk/ data_request/ cif*.

The quantitative energy-dispersive X-ray spectroscopy (EDX, JEOL-SEM, JSM-6700F) analysis of the crystals shows the presence of elements K, Sb, and Pd with the roughly expected ratios.(See Figure S3.1) In intermetalloid cluster **1**, the ratio of K/Sb/Pd is near 4/12/21, while K/Sb/Pd ratio is roughly 3/12/21 of **2**.

S2 A detailed structural comparison between 1 and 2

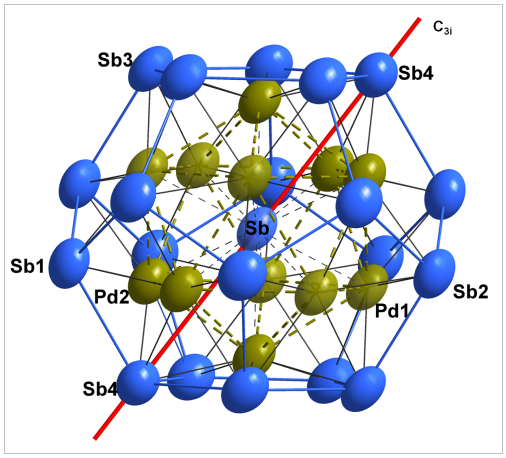

Fig. S2.1. The structure of $[Sb@Pd_{12}@Sb_{20}]^{3-}$ (**2a**)(50% probability for thermal ellipsoids) with C_{3i} axis in red

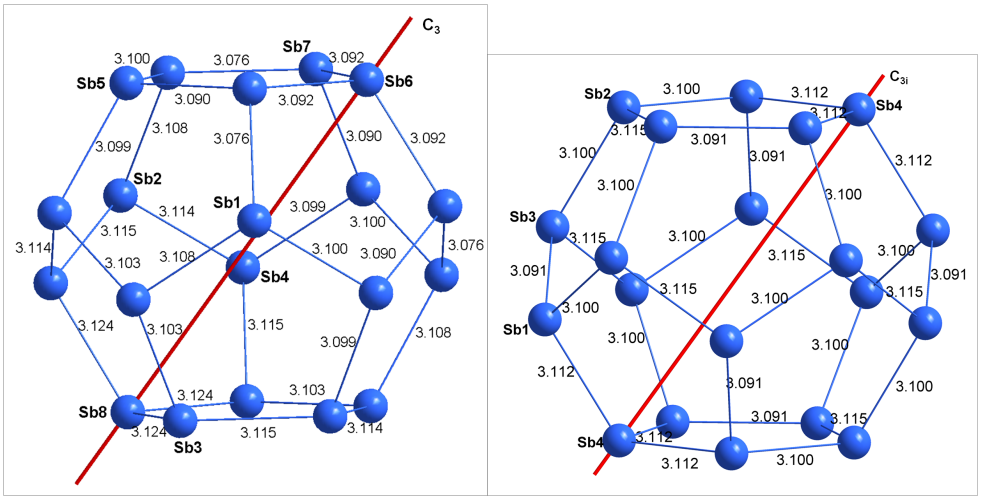

1a **2a**

Fig. S2.2. Sb–Sb distances of the Sb_{20} in $[Sb@Pd_{12}@Sb_{20}]^{4-}$(**1a**) with *av*. 3.104(2) Å and **in** $[Sb@Pd_{12}@Sb_{20}]^{3-}$ (**2a**) with *av*. 3.102(2) Å

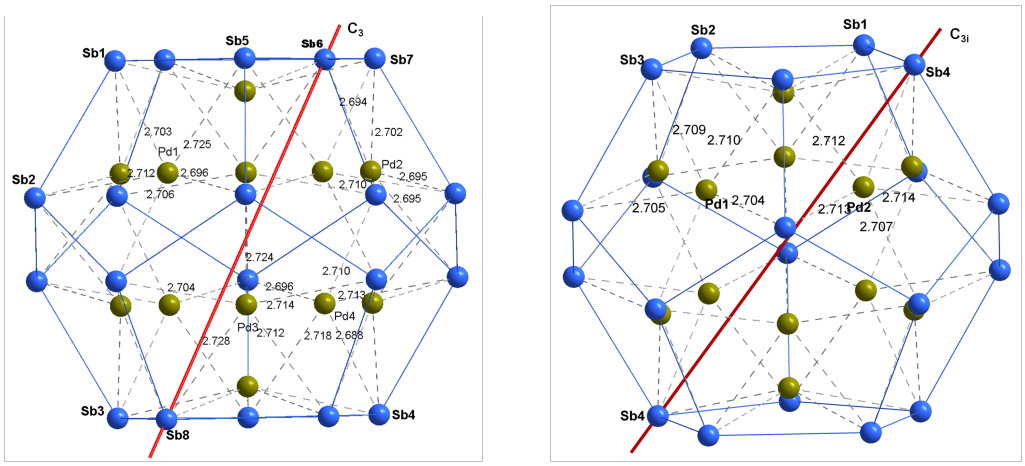

1a **2a** (av.)

Fig. S2.3. Sd—Pd bond lengths in $[Sb@Pd_{12}@Sb_{20}]^{4-}$ (**1a**) with *av*. 2.707(2) Å and in $[Sb@Pd_{12}@Sb_{20}]^{3-}$ (**2a**) with **av**. 2.709(2) Å

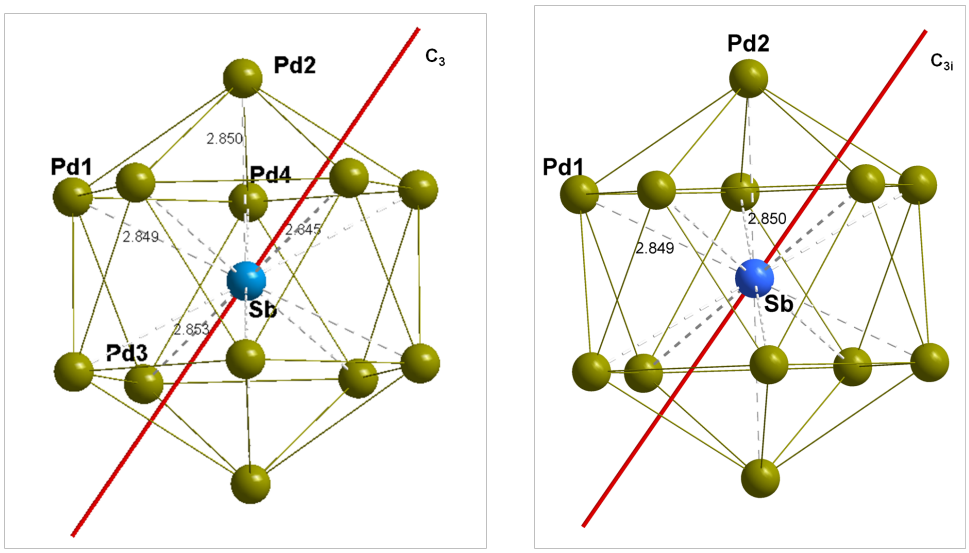

1a **2a**

Fig. S2.4. Sb–Pd distances of the [Sb@Pd_{12}] unit in [Sb@Pd_{12}@Sb_{20}]$^{4-}$ (**1a)** with *av*. 2.849(2) Å and in [Sb@Pd_{12}@Sb_{20}]$^{3-}$ (**2a**) with *av*. 2.850(2) Å.

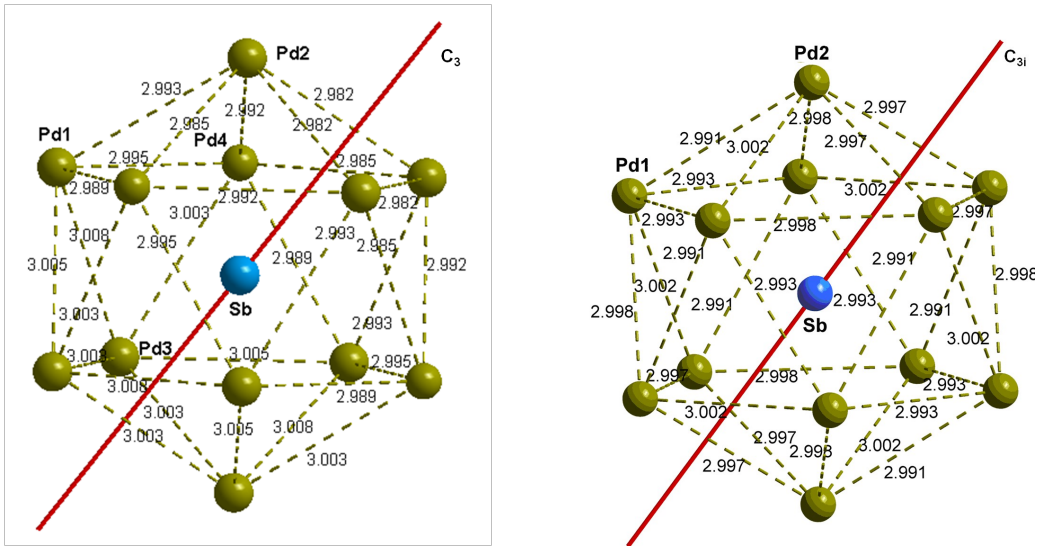

1a **2a**

Fig. S2.5. Pd–Pd distances in [Sb@Pd_{12}@Sb_{20}]$^{4-}$ (**1a)** with *av*. 2.996(2) Å and [Sb@Pd_{12}@Sb_{20}]$^{3-}$ (**2a**) with *av*. 2.997(2) Å

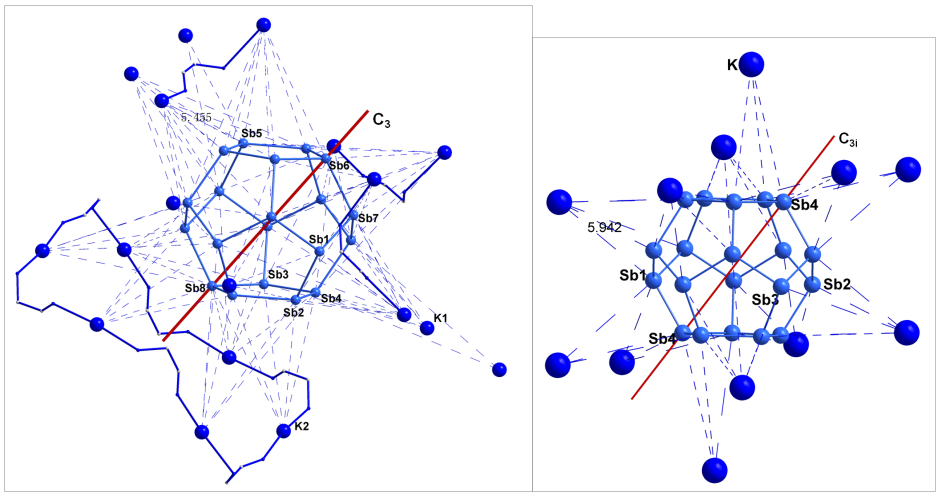

a b

Fig. S2.6. (**a**, left)Extensive $[Sb_{20}]^{-}$–K18 interactions in $[Sb@Pd_{12}@Sb_{20}][K(18\text{-crown-}6)]_4$•3en(**1**•3en), six K atoms are connected by six en molecules into a thirty-membered ring. (**b,** right) Extensive $[Sb_{20}]$–K12 interactions in $[Sb@Pd_{12}@Sb_{20}][K(2,2,2\text{-cryptand})]_3$ with a three-fold rotation axis drawn in a red line.

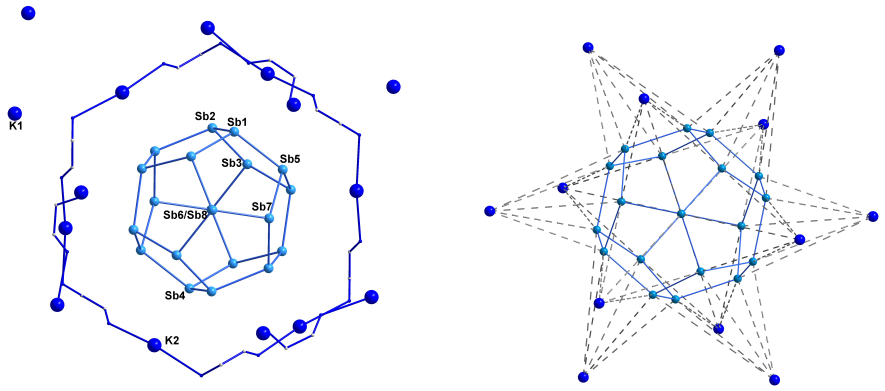

a b

Fig. S2.7. (**a**, left) Arrangement of 18 K atoms surrounding $[Sb_{20}Pd_{12}@Sb]^{4-}$ (**1a**) in **1a**•$[K(18\text{ crown-}6)]_4$•3en viewed down three-fold rotation axis. Six K atoms are connected by six en molecules into a thirty-membered ring. (**b**, right) Arrangement of 12 K atoms surrounding $[Sb_{20}Pd_{12}@Sb]^{3-}$ (**2a**) in **2a**•$[K(2,2,2\text{-crypt})]_3$ viewed down three-fold rotation axis.

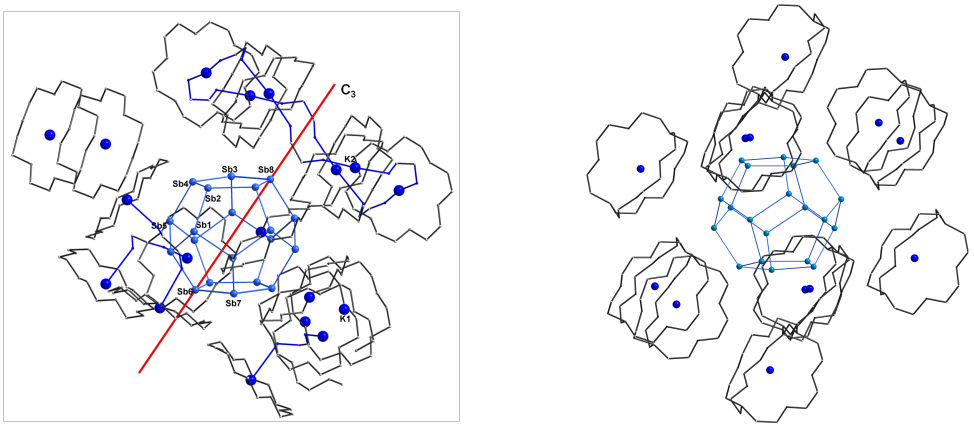

a b

Fig. S2.8 (a, left) arrangement of 18 $[K(18\text{-crown-}6)]^{+}$ ions surrounding $[Sb_{20}]$ in **1 (b, right)** arrangement of 12 $[K(2,2,2\text{-crypt})]^{+}$ ions surrounding $[Sb_{20}]$ in **2. a** and **b** are drawn with their 3-fold axis along the same orientation.

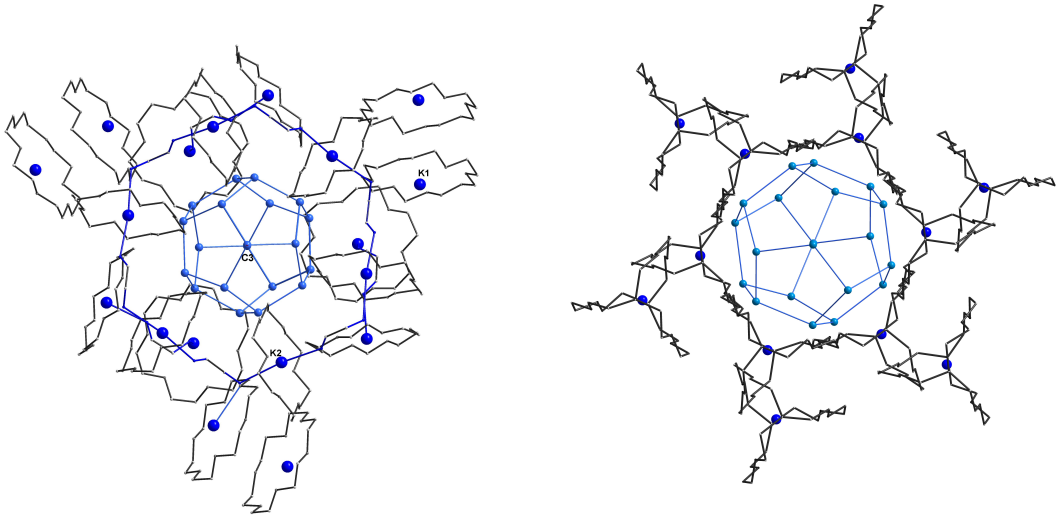

a **b**

Fig. S2.9 (**a,** left) arrangement of 18 $[K(18\text{-crown-}6)]^+$ ions surrounding $[Sb_{20}]$ in **1.** (**b,** right) arrangement of 12 $[K(2,2,2\text{-crypt})]^+$ ions surrounding $[Sb_{20}]$ in **2.** **a** and **b** are drawn with 3-fold axis viewed down.

Table S2.1. Sb•••K separations (Å) in **1**.

Atoms	Distance (Å)
Sb1-K2	5.455
Sb1-K2	6.453
Sb1-K1	8.557
Sb2-K2	6.314
Sb2-K2	7.936
Sb2-K2	8.104
Sb3-K2	7.063
Sb3-K2	7.253
Sb3-K2	8.518
Sb3-K1	8.739
Sb4-K2	7.156
Sb4-K1	7.359
Sb4-K2	7.709
Sb5-K2	6.452
Sb5-K1	7.233
Sb5-K2	7.845
Sb5-K2	8.107
Sb6-K2	7.200
Sb7-K2	6.559
Sb7-K2	6.894
Sb7-K2	6.954
Sb8-K2	8.111
Sb8-K2	8.479
average Sb-K	7.430

Table S2.2. Sb•••K separations (Å) in **2**

Atoms	Distance (Å)
Sb1-K	6.283
Sb1-K	7.423
Sb1-K	7.473
Sb2-K	5.942
Sb2-K	7.495
Sb3-K	6.761
Sb3-K	7.235
Sb4-K	7.268
sverage Sb-K	6.985

S3 EDX spectroscopy of 1 and 2

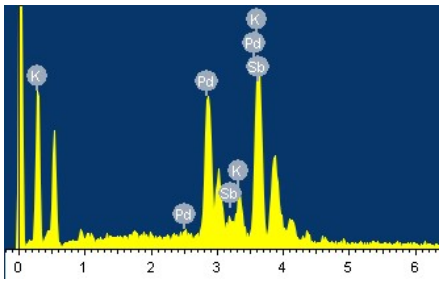

Element	Weight	Atom %
K	4.02	11.06
Pd	32.12	32.48
Sb	63.87	56.45
Total	100.00	100%

1

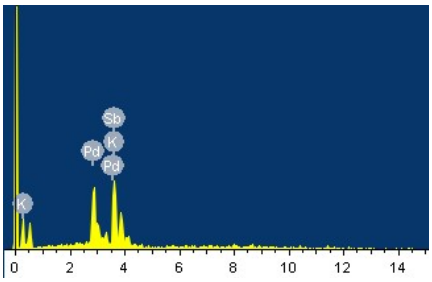

Element	Weight	Atoms %
K	3.00	8.42
Pd	32.70	33.69
Sb	64.30	57.89
Total	100.00	100%

2

Fig. S3.1. EDX spectroscopy of **1** and **2**.

S4 EPR spectrum of 1

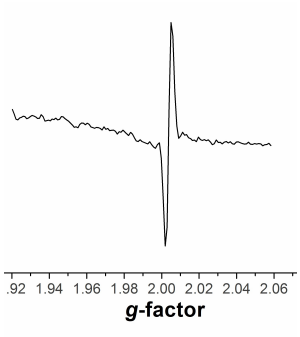

Fig. S4.1. EPR spectrum of a crystalline sample of **1**.

S5 Computational result analyses

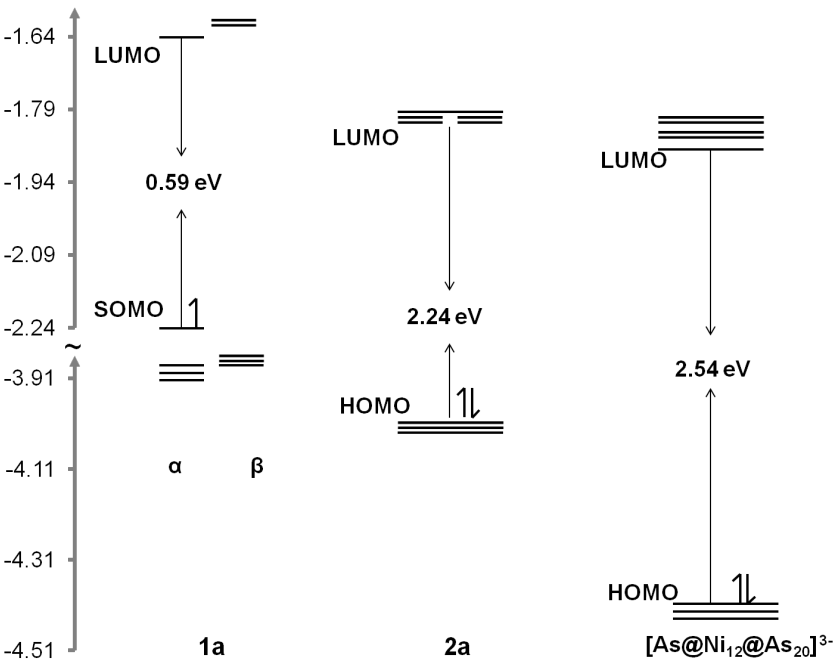

Fig. S5.1. Molecular orbital energy diagram of **1a**, **2a** and $[As@Ni_{12}@As_{20}]^{3-}$ [8].

Table S5.1 Molecular orbital composition analysis by the natural atomic orbital (NAO) method for **1a** and **2a**.

1a ($[Sb@Pd_{12}@Sb_{20}]^{4-}$)		**2a** ($[Sb@Pd_{12}@Sb_{20}]^{3-}$)	
HOMO-1(alpha)		**HOMO-1**	
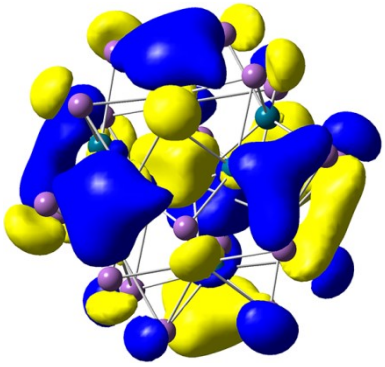		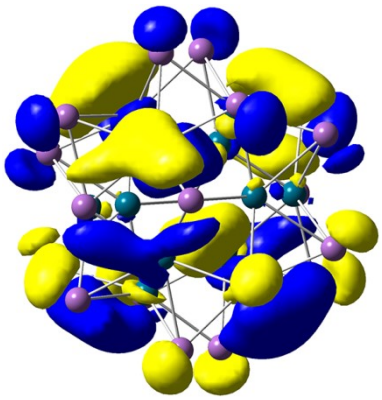	
Atoms	**composition**	**Atoms**	**composition**
Sb1	8.87%	Sb1	9.71%
Pd2	0.47%	Pd2	0.78%
Pd3	2.05%	Pd3	3.02%
Pd4	0.48%	Pd4	5.25%
Pd5	0.46%	Pd5	0.50%
Pd6	0.48%	Pd6	1.35%
Pd7	1.96%	Pd7	2.46%
Pd8	2.09%	Pd8	2.37%
Pd9	4.76%	Pd9	0.50%
Pd10	4.58%	Pd10	1.26%
Pd11	4.26%	Pd11	0.76%
Pd12	1.94%	Pd12	3.02%
Pd13	4.44%	Pd13	5.31%
Sb14	3.39%	Sb14	3.45%
Sb15	3.19%	Sb15	3.29%
Sb16	3.34%	Sb16	3.44%
Sb17	3.21%	Sb17	2.85%
Sb18	2.98%	Sb18	3.56%
Sb19	3.23%	Sb19	2.78%
Sb20	3.28%	Sb20	3.49%
Sb21	3.26%	Sb21	2.69%
Sb22	2.95%	Sb22	3.49%
Sb23	3.24%	Sb23	3.32%
Sb24	3.48%	Sb24	2.96%
Sb25	3.00%	Sb25	2.51%
Sb26	3.47%	Sb26	3.20%
Sb27	3.08%	Sb27	2.65%
Sb28	3.16%	Sb28	3.05%
Sb29	2.99%	Sb29	3.17%

Sb30	3.11%	Sb30	2.97%
Sb31	2.82%	Sb31	3.88%
Sb32	2.90%	Sb32	3.33%
Sb33	2.80%	Sb33	3.38%

Fragments	**composition**	**Fragments**	**composition**
Sb-center	8.87%	Sb-center	9.71%
Sb_{20}	62.88%	Sb_{20}	63.46%
Pb_{12}	27.97%	Pb_{12}	26.58%

SOMO(alpha)

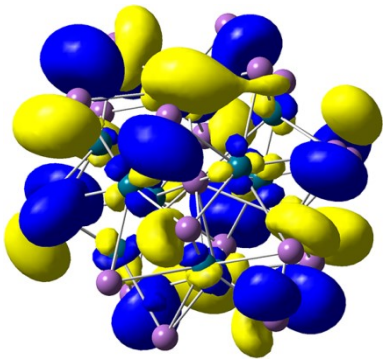

HOMO

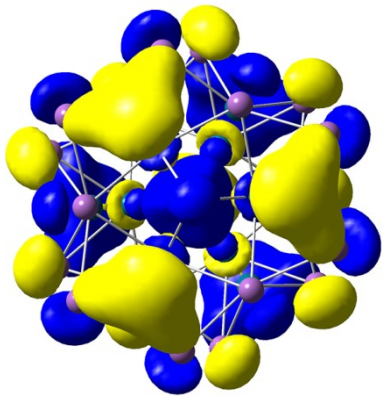

Atoms	**composition**	**Atoms**	**composition**
Sb1	0.02%	Sb1	9.87%
Pd2	2.85%	Pd2	0.71%
Pd3	0.49%	Pd3	0.55%
Pd4	2.38%	Pd4	0.67%
Pd5	2.33%	Pd5	3.72%
Pd6	2.77%	Pd6	4.14%
Pd7	0.57%	Pd7	3.81%
Pd8	0.35%	Pd8	3.76%
Pd9	0.92%	Pd9	3.67%
Pd10	0.92%	Pd10	4.07%
Pd11	0.70%	Pd11	0.59%
Pd12	0.40%	Pd12	0.45%
Pd13	0.78%	Pd13	0.55%
Sb14	6.18%	Sb14	3.34%
Sb15	0.66%	Sb15	3.64%
Sb16	1.00%	Sb16	3.22%
Sb17	2.99%	Sb17	3.44%
Sb18	2.39%	Sb18	2.89%
Sb19	4.01%	Sb19	3.28%
Sb20	5.15%	Sb20	3.58%
Sb21	2.34%	Sb21	3.28%
Sb22	7.74%	Sb22	3.48%

Sb23	5.55%	Sb23	2.98%
Sb24	0.99%	Sb24	3.31%
Sb25	3.90%	Sb25	3.65%
Sb26	6.30%	Sb26	3.26%
Sb27	4.05%	Sb27	3.44%
Sb28	0.59%	Sb28	2.91%
Sb29	3.14%	Sb29	2.96%
Sb30	2.14%	Sb30	2.89%
Sb31	6.68%	Sb31	2.34%
Sb32	10.21%	Sb32	2.88%
Sb33	7.80%	Sb33	2.42%

Fragments	**composition**	**Fragments**	**composition**
Sb-center	0.02%	Sb-center	9.87%
Sb_{20}	83.79%	Sb_{20}	63.19%
Pb_{12}	15.47%	Pb_{12}	26.68%

LUMO(alpha)

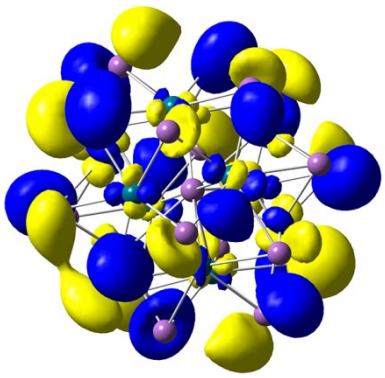

LUMO

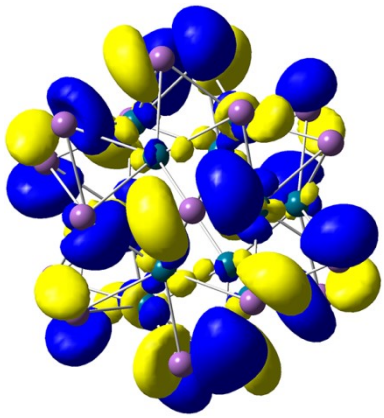

Atoms	**composition**	**Atoms**	**composition**
Sb1	0.01%	Sb1	0.03%
Pd2	0.96%	Pd2	1.95%
Pd3	2.96%	Pd3	2.26%
Pd4	1.60%	Pd4	0.52%
Pd5	1.59%	Pd5	1.44%
Pd6	0.97%	Pd6	0.67%
Pd7	2.88%	Pd7	0.88%
Pd8	1.07%	Pd8	0.83%
Pd9	0.59%	Pd9	1.20%
Pd10	0.71%	Pd10	0.58%
Pd11	0.73%	Pd11	1.87%
Pd12	0.86%	Pd12	2.09%
Pd13	0.52%	Pd13	0.49%
Sb14	1.75%	Sb14	0.29%
Sb15	5.69%	Sb15	4.91%

Sb16	4.38%	Sb16	3.27%
Sb17	7.43%	Sb17	3.88%
Sb18	3.83%	Sb18	3.72%
Sb19	3.95%	Sb19	3.57%
Sb20	1.76%	Sb20	3.91%
Sb21	4.09%	Sb21	6.29%
Sb22	2.18%	Sb22	0.23%
Sb23	0.30%	Sb23	1.41%
Sb24	6.16%	Sb24	4.48%
Sb25	3.50%	Sb25	6.70%
Sb26	0.24%	Sb26	4.75%
Sb27	5.41%	Sb27	3.39%
Sb28	4.23%	Sb28	5.97%
Sb29	4.91%	Sb29	1.76%
Sb30	6.77%	Sb30	6.71%
Sb31	1.78%	Sb31	8.09%
Sb32	8.40%	Sb32	4.33%
Sb33	7.00%	Sb33	6.83%
Fragments	**composition**	**Fragments**	**composition**
Sb-center	0.01%	Sb-center	0.03%
Sb_{20}	83.75%	Sb_{20}	84.49%
Pb_{12}	15.44%	Pb_{12}	14.78%

Table S5.2 Calculated spin density and atomic spin population for **1a**.

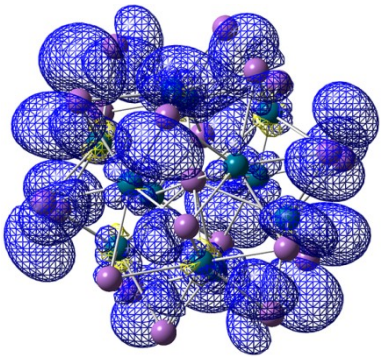

Atom	Alpha_population	Beta_ population	Spin_ population
Sb1	1.56353	1.57500	-0.01147
Pd2	9.60000	9.56100	0.03900
Pd3	9.56744	9.57226	-0.00483
Pd4	9.59716	9.56544	0.03172
Pd5	9.59701	9.56652	0.03049
Pd6	9.60075	9.56341	0.03734
Pd7	9.56710	9.57156	-0.00446

Pd8	9.56134	9.56772	-0.00638
Pd9	9.55472	9.55291	0.00181
Pd10	9.55484	9.55219	0.00266
Pd11	9.57033	9.57089	-0.00056
Pd12	9.57240	9.58082	-0.00842
Pd13	9.56951	9.56985	-0.00034
Sb14	2.34759	2.27459	0.07300
Sb15	2.29249	2.29860	-0.00611
Sb16	2.29423	2.29774	-0.00351
Sb17	2.30498	2.29455	0.01043
Sb18	2.30246	2.28716	0.01530
Sb19	2.32505	2.28549	0.03956
Sb20	2.33549	2.27650	0.05898
Sb21	2.30419	2.29195	0.01224
Sb22	2.37356	2.26203	0.11153
Sb23	2.33271	2.27189	0.06082
Sb24	2.29870	2.30004	-0.00133
Sb25	2.32235	2.28266	0.03969
Sb26	2.34140	2.27270	0.06870
Sb27	2.31807	2.28856	0.02952
Sb28	2.28666	2.29544	-0.00878
Sb29	2.31054	2.28732	0.02322
Sb30	2.29961	2.29251	0.00711
Sb31	2.35989	2.26333	0.09656
Sb32	2.40623	2.25430	0.15193
Sb33	2.36766	2.25304	0.11461

Fragments	**Sum of Spin_ population**
Sb_{20}	0.89347
Pb_{12}	0.11803

S6 References

1 a) W. Hönle, H. G. von Schnering, *Zeitschrift für Kristallographie-Crystalline Materials*, 1981, **155**, 307. b) K. Seifert-Lorenz, J. Hafner, *Physical Review B*, 1999, **59**, 829.

2 Gaussian 09, Revision D.01, M. J. Frisch, G. W. Trucks, H. B. Schlegel, G. E. Scuseria, M. A. Robb, J. R. Cheeseman, G. Scalmani, V. Barone, B. Mennucci, G. A. Petersson, H. Nakatsuji, M. Caricato, X. Li, H. P. Hratchian, A. F. Izmaylov, J. Bloino, G. Zheng, J. L. Sonnenberg, M. Hada, M. Ehara, K. Toyota, R. Fukuda, J. Hasegawa, M. Ishida, T. Nakajima, Y. Honda, O. Kitao, H. Nakai, T. Vreven, J. A. Montgomery, Jr., J. E. Peralta, F. Ogliaro, M. Bearpark, J. J. Heyd, E. Brothers, K. N. Kudin, V. N. Staroverov, R. Kobayashi, J. Normand, K. Raghavachari, A. Rendell, J. C. Burant, S. S. Iyengar, J. Tomasi, M. Cossi, N. Rega, J. M. Millam, M. Klene, J. E. Knox, J. B. Cross, V. Bakken, C. Adamo, J. Jaramillo, R. Gomperts, R. E. Stratmann, O. Yazyev, A. J. Austin, R. Cammi, C. Pomelli, J. W. Ochterski, R. L. Martin, K. Morokuma, V. G. Zakrzewski, G. A. Voth, P. Salvador, J. J. Dannenberg, S. Dapprich, A. D. Daniels, Ö. Farkas, J. B. Foresman, J. V. Ortiz, J. Cioslowski, and D. J. Fox, Gaussian, Inc., Wallingford CT, 2009.

3 A. D. Becke, *J. Chem. Phys*. 1993, **98**, 5648.

4 C. Lee, W.Yang , R.G . Parr, *Phys. Rev. B.* 1988, **37**, 785.

5 a) M. Cossi, G. Scalmani, N. Rega, V. Barone, *J. Chem. Phys.* 2002**,** 117, 43; b) V. Barone, M. Cossi, J. Tomasi, *J. Chem. Phys*. 1997**, 107**, 3210.

6 a) T. Lu and F. Chen, *J Comput Chem*, 2012, **33**, 580. b) J. Mol. Graph. Model., 2012, **38**, 314. c) Multiwfn software can be freely downloaded from website: http://multiwfn.codeplex.com/.

7 G. M. Sheldrick, SHELXTL, version 6.21; Bruker-Nonium AXS: Madison, WI, 2001.

8 M. J. Moses, J. C. Fettinger and B. W. Eichhorn, *Science.* 2003, **300**, 778.